KEYWORDS: thermoelectric generator, selective laser melting, powder spreading, powder morphology

Energy Materials Analysis for Additive Manufacturing by Selective Laser Melting

RACHEL GRAY[1], DEVIN JESSUP[2], AND SANIYA LEBLANC[3]

1 MECHANICAL ENGINEERING, SEAS '20, rachelgray97@gwu.edu **2** ELECTRICAL ENGINEERING, SEAS '19
3 ASSISTANT PROFESSOR OF MECHANICAL AND AEROSPACE ENGINEERING

ABSTRACT

This research aimed to improve selective laser melting (SLM) of energy materials for thermoelectric power generation devices. Thermoelectric generators (TEG) are solid state devices that offer the potential for waste heat recovery in combustion and heat process systems. These devices are currently being manufactured using bulk material processing with many integration and assembly steps, leading to decreased product efficiency and high manufacturing costs. Selective laser melting is an additive manufacturing technique, when combined with semiconductive powder offers a solution to these manufacturing challenges.

INTRODUCTION

Thermoelectric generators are devices which convert waste heat from various heat systems into usable electricity. As seen in Fig 1, on average combustion and heat systems lose 66% of their energy to waste heat. Thermoelectric materials work via the Seebeck effect, wherein a temperature difference across the material causes electrical charge carriers to move, producing an electric voltage. Current advances in thermoelectric materials have not resulted in efficient and economically viable devices due to manufacturing challenges. The current manufacturing process, as illustrated in Fig 2, requires many steps before assembly. These steps not only create a time-intensive process, they also provide limited geometries (rectangular legs only) which fail to effectively capture waste heat from curved heat systems. The bulk material processing technique of dicing also causes 50% of the material to be wasted.

The additive manufacturing technique of selective laser melting, as depicted in Fig 3, eliminates the multi-step process currently required for making thermoelectric legs. The laser's ability to move in a range of patterns allows for a variety of geometric shapes, compatible with many heat sources, to be created. In addition, excess material can be recycled for use in the manufacturing of the next device (El-Desouky, Carter, Mahmoudi, Elwany, and LeBlanc, 2017).

In selective laser melting, a thin layer of powder is scanned over by a laser in a desired pattern, sintering the powder particles together. Another layer of powder is spread, and the process is repeated until the desired structure is formed. The remaining powder is then removed and recycled for the next device. This process, however, requires specific starting powder characteristics (desired particle distribution, and high levels of circularity and convexity).

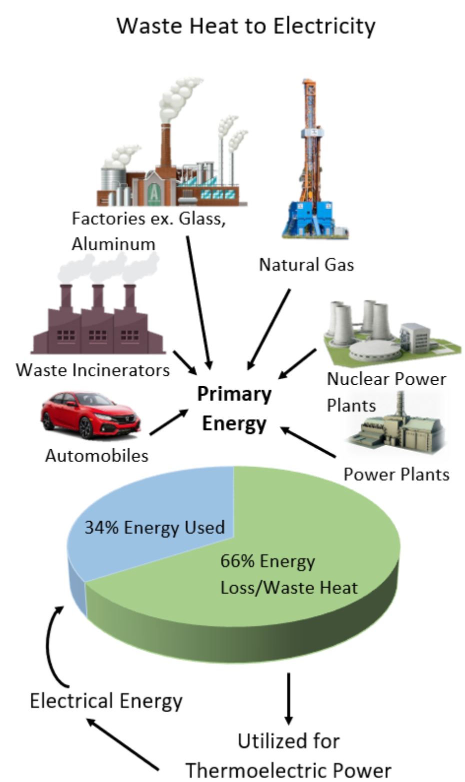

FIGURE 1. *Examples of heat and combustion systems which on average lose 66% of their energy to waste heat (Joly et al., n.d.)*

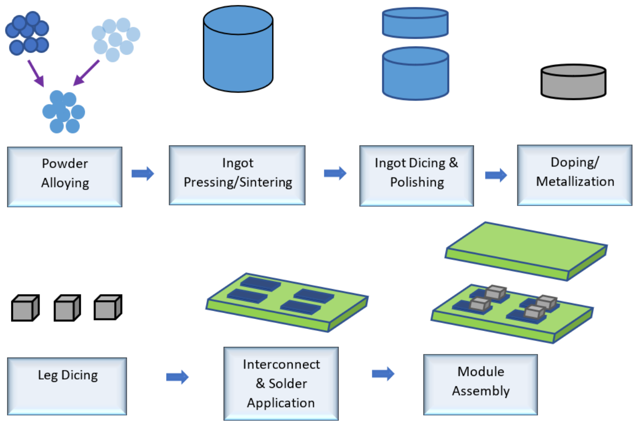

FIGURE 2. *Typical steps for traditional manufacturing of thermoelectric devices (LeBlanc, 2014)*

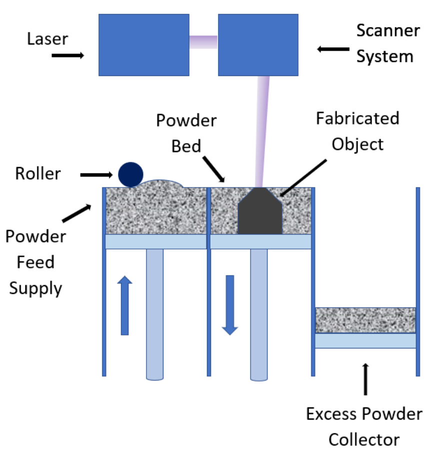

FIGURE 3. *Schematic of Selective Laser Melting approach, eliminating dicing and assembly steps, and allowing desired geometries (Leinenbach, n.d.)*

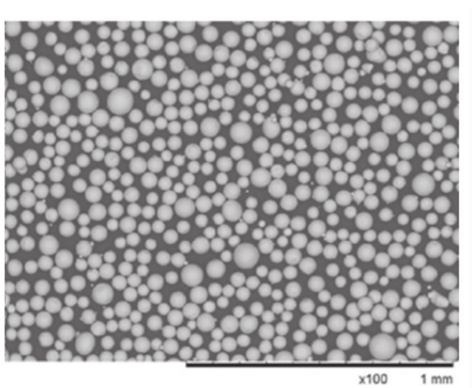

FIGURE 4. *Image of optimal powder profile: high values of circularity, convexity, and desired powder distribution (Triantaphyllou, Giusca, Macaulay, Roerig, Hoebel, Leach, Tomita, and Milne, 2015)*

FLOWABILITY

Flowability is multidimensional and depends on many powder characteristics. Because of this, it is important to look at many measurements when assessing the flowability of a powder. These measurements include angle of repose, angle of spatula, compressibility, and cohesiveness or uniformity coefficient. These parameters are factored into a single flowability index (Schuck, Jeantet, and Dolivet, 2012). Flowability not only affects how powder spreads through a device, it also impacts the end TEG product. Powder parameters such as convexity, circularity, and particle size distribution all affect the density of the end TEG device. With a higher density, a TEG is more efficient and is more resilient to internal fractures. If particles are elongated and nonuniform, it leads to an increase in particle friction and possible particle interlocking which in return decreases flowability. These characteristics also decrease the final density as they can lead to uneven sintering and interlayer voids, which cause internal fractures (El-Desouky, Carter, Mahmoudi, Elwany, and LeBlanc, 2017).

The Spiering's (Fig 5) and the Karapatis (Fig 6) requirements create a suitable size distribution for both flowability and density. The Karapatis requirement states that fifty percent of particles are ten times coarser than ten percent of the finest grains, and about twenty percent of the particles are in a one to twenty ratio. Spiering's requirements state that effective layer thickness is at least fifty percent higher than the diameter of ninety percent of the powder particles and that there are a sufficient number of fine particles to fill the voids between the courser. Also, particles below 5-6µm in diameter will cause agglomeration which will decrease flowability and decrease the part density (Spierings and Levy, 2009).

$$\frac{D_{90}}{D_{10}} \approx 5 \quad \frac{t_{eff}}{D_{90}} \approx 1.5$$

FIGURE 5. *Spiering's requirements for suitable size distribution (Spierings and Levy, 2009)*

$$D_{90} < t_{Layer} \qquad \frac{D_{50}}{D_{10}} \geq 10 \qquad \frac{D_{90}}{D_{10}} \leq 19$$

FIGURE 6. *Karapatis requirements for suitable size distribution (Spierings and Levy, 2009)*

POWDER SPREADING

The creation of a powder spreading rig (PSR) was needed in the lab to automate the previous system of hand-rolling each powder layer in the SLM process, as well as to obtain repeatable powder layers. The design of the powder spreading rig was modeled after current SLM designs and utilizes a 3D printer.

The base plate at the center of the 3D printer acts as the powder bed where sintering occurs. It uses the axial controls of the 3D printer to move downward in the z axial direction in increments desired, as small as 20μm. On the left side of the base plate is a box that houses the powder. The powder moves upward in the z axial direction by use of an additional motor which is controlled by an Arduino. The Arduino is programmed in C and allows for equal incremental movement as the base plate. On the right-hand side is a box that captures the excess powder, which can then be reused. The rolling system utilizes the axial controls of the 3D printer as well, and these controls were reprogrammed in G-code. All circuits are controlled either by a SDS card or through a USB cable. This allows the PSR to work in an inert gas bubble, which is necessary for many energy materials.

The PSR starts with the roller in the back-left hand corner. The powder is raised to the desired level and the roller begins moving along the positive x-axis and then along the positive y-axis. This rolls the powder onto the powder bed, pushing any excess powder into the right-hand container. The roller then retraces back along its path and pauses in its starting position, allowing the lasering to take place. Once the lasering is complete the PSR will lower by the same desired increment, and the process will repeat for the desired number of layers.

One problem that is foreseeable is the current desired layer size, which is 50μm. It is unclear whether the powders ability to flow will allow this small layer size.

BALL MINING

One method to improve flowability is ball milling. In this research, a high energy ball mill is used. Parameters such as ball to powder ratio, grinding speed and duration, as well as pause intervals are varied in order to find an optimal set of parameters. The combined centrifugal and centripetal force creates a powerful impact force, which should improve the overall shape of the powder, and potentially the flowability. The powder was milled in an argon atmosphere to decrease oxidation and was milled at room temperature. The powder will be analyzed based on the previously discussed flowability measurements as well as through an image analysis software.

IMAGING

To establish an imaging and analysis technique bismuth telluride, a semi conductive powder in the TEG field was used. To characterize the powder, light microscopy was utilized to produce images. A 10X magnification was found to be most effective in balancing the glare against particles with an appropriate focus of both large and small particles. Mounting the powder on the slides for imaging required 30.0 mL of ethylene glycol with 0.25 grams of bismuth telluride. This suspension was then spin coated onto glass slides at different speeds for various times.

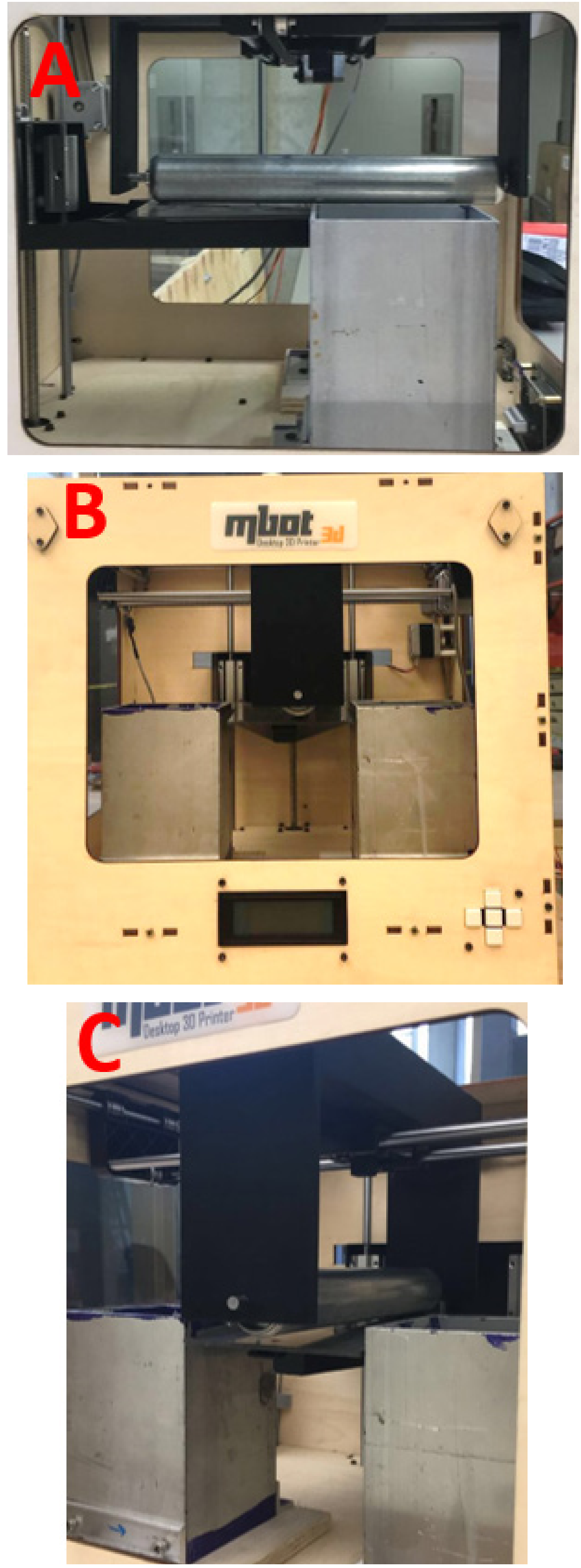

FIGURE 7. ***A.*** *a side view,* ***B.*** *a front view and* ***C.*** *an angled front view of the powder spreading rig*

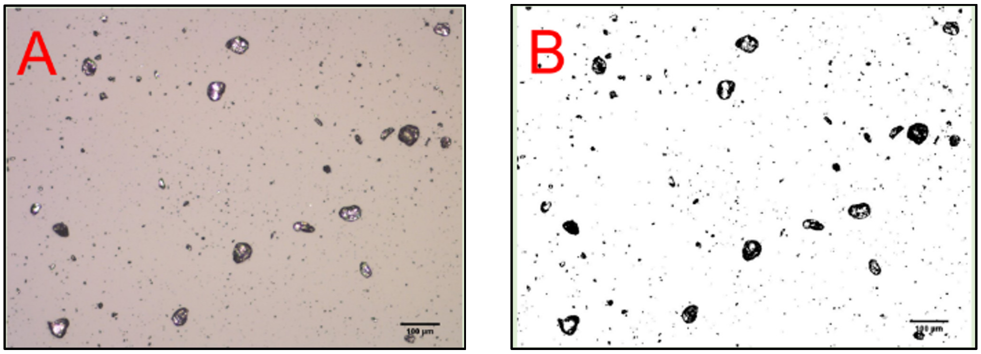

FIGURE 8. ***A.*** *bismuth telluride at 10x magnification.* ***B.*** *the powder post-process, as a black and white mask*

PROGRAM

Once the images were acquired, they were all processed through an ImageJ software derivative called Fiji Is Just ImageJ (FIJI) (Schindelin, Arganda-Carreras, Frise, et al., 2012). In the program, each image was converted to 8-bit greyscale and then its contrast was enhanced. Following this, a mask was applied over the image, inverting the look-up table (LUT) and producing a flat black and white image. Additionally, scale was applied to each image in microns. Utilizing the black and white image, the particles were then analyzed to obtain values for area, perimeter, Ferret's diameter, and convex hull perimeter. To obtain the convex hull perimeter, a plugin was applied to FIJI called "Shape Filter" (Wagner and Lipinski, 2013). A macro was utilized to automate the process and to help control for human error. An area threshold of 30 µm was established for each image, to remove particles which would be too small for effective use in SLM and which would interfere with program analysis methods. This process can be seen in Fig 8.

MORPHOLOGY RESULTS

Magnesium silicide stannide is an off-the-shelf semiconductive powder with a high operating temperature. It was examined to determine its ability to be used in SLM. A set of data was first taken on un-ball milled magnesium silicide stannide to establish a preliminary set of data, for use in later comparison.

Circularity, which is a ratio of how elongated or circular a particle is, is set on a scale from zero to one. One being the most circular and zero being the most oblong. Unmilled magnesium silicide stannide averaged 0.6 in circularity as depicted in Fig 9. This number is relatively low and will need to be improved greatly before magnesium silicide stannide can be utilized in the SLM process.

Particle size distribution looks at the different sizes in particles that are represented in a sample. This measurement is based on Ferret's diameter which is the longest diameter at any point on the particle. Unmilled magnesium silicide stannide had a wide range of particle sizes as seen in Fig 10. This range was between 5µm and 375 µm, with the average being 25 µm. The powder can go through a sieving process to extract the exact sizes as determined by the user.

Convexity is a ratio of how abstract a particles parameter is. It as well is on a scale from zero to one: zero being very abstract with many sharp edges and points, and one being perfectly round and smooth. Unmilled magnesium silicide stannide averaged 0.9 in convexity as shown in Fig 11. This number is relatively high and should help aid the particles in flowing through the powder spreading system, however, could still be improved.

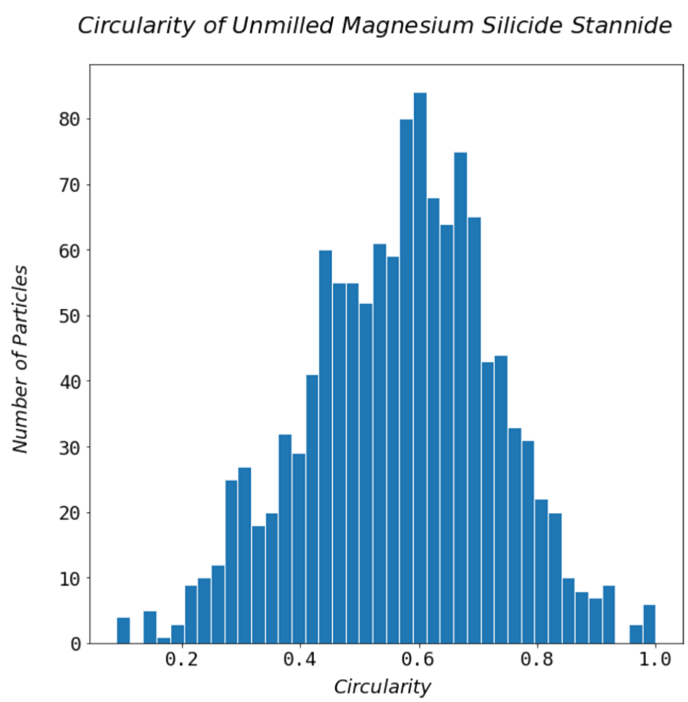

FIGURE 9. *A graph of the overall circularity values, the average being around 0.6*

CONCLUSION AND FUTURE WORK

This work shows that FIJI is a free and robust software for use with examining powder morphology, providing results with a high degree of repeatability. Unmilled magnesium silicide stannide has mid-range values for circularity and relatively high values for convexity. These properties will reduce flowability and compromise powder bed density. More work will need to be done to improve these powder properties before magnesium silicide stannide can be used in the SLM process.

A procedure to ensure repeatability and reliability of the powder spreading rig in creating uniform layers of thickness will need to be developed. And a stronger relationship between flowability and powder morphology will need to be established before SLM can be implemented in the TEG manufacturing process.

ACKNOWLEDGEMENTS

The researchers would like to thank Haidong Zhang and Michael Orrill for their expertise and help throughout the project. William Rutkowski and the machine shop for help building the PSR. Additional thanks go to the National Science Foundation for enabling the Nanotechnology Fellow's Program with Award EEC-1446001.

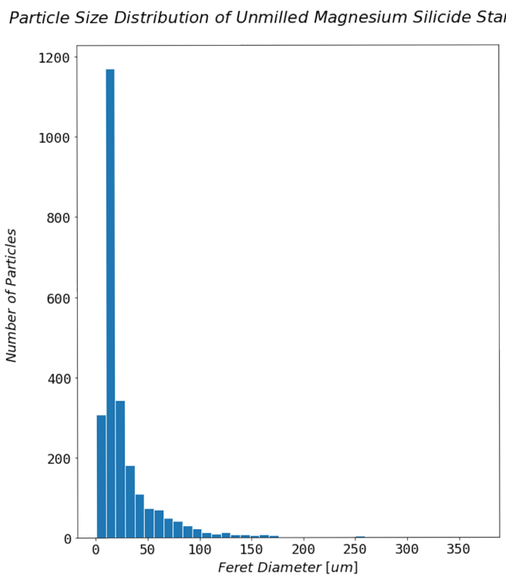

FIGURE 10. *A graph of overall particle size distribution. Particles ranged from 5μ to 375 μm, with the average being around 25μm.*

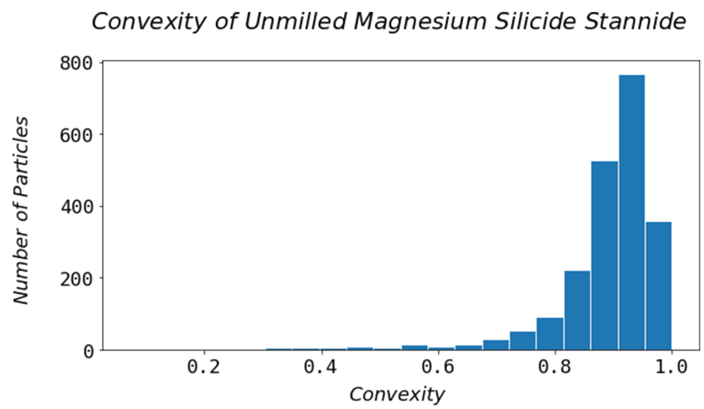

FIGURE 11. *A graph of the overall convexity, with the average being around 0.9*

REFERENCES

1. A.B. Spierings, and G. Levy, "Comparison of density of stainless steel 316L parts produced with selective laser melting using different powder grades," in Solid Freeform Fabrication Symposium, Austin, TX, 2009, pp. 1-12.
2. Ahmed El-Desouky, Michael Carter, Mohamed Mahmoudi, Alaa Elwany, Saniya LeBlanc. "Influences of energy density on microstructure and consolidation of selective laser melted bismuth telluride thermoelectric powder". *Journal of Manufacturing Processes*, vol. 25, pp. 411-417, 2017.
3. Joly, Clement, et al. "Waste Heat Recovery Technologies |." *Turbomachinery Blog*, blog.softinway.com/en/tag/waste-heat-recovery-technologies/.
4. Leinenbach, Christian. "Selective Laser Melting ." *Empa - Coating Competence Center - Selective Laser Melting* (SLM), www.empa.ch/web/coating-competence-center/selective-laser-melting.
5. Pierre Schuck, Romain Jeantet, Anne Dolivet, "Ch. 8 Determination of Flowability and Floodability Indices," in *Analytical Methods for Food and Dairy Powder*, ed 1: John Wiley & Sons Inc., 2012, ch. 8, pp. 129-136.
6. Saniya LeBlanc. "Thermoelectric generators: Linking material properties and systemsengineering for waste heat recovery applications". *Sustainable Materials and Technologies*, 2014. http://dx.doi.org/10.1016/j.susmat.2014.11.002
7. Schindelin, J.; Arganda-Carreras, I. & Frise, E. et al. (2012), "Fiji: an open-source platform for biological-image analysis", *Nature methods*9(7): 676-682, PMID 22743772, doi:10.1038/nmeth.2019 (on Google Scholar).
8. Triantaphyllou, Andrew & Giusca, Claudiu & Macaulay, Gavin & Roerig, Felix & Hoebel, Matthias & Leach, Richard & Tomita, Ben & Milne, Katy. (2015). Surface texture measurement for additive manufacturing. Surface Topography: Metrology and Properties. 3. 024002. 10.1088/2051-672X/3/2/024002.
9. Wagner, T and Lipinski, H 2013. IJBlob: An ImageJ Library for Connected Component Analysis and Shape Analysis. Journal of Open Research Software 1(1):e6, DOI: http://dx.doi.org/10.5334/jors.ae